THE JOURNAL OF PHYSICAL CHEMISTRY Letters

Letter

Cite This: J. Phys. Chem. Lett. 2018, 9, 4059−4065

pubs.acs.org/JPCL

Site-Specific Hydrogen Exchange in a Membrane Environment Analyzed by Infrared Spectroscopy

Esther S. Brielle* and Isaiah T. Arkin*

The Alexander Silberman Institute of Life Sciences, Department of Biological Chemistry, The Hebrew University of Jerusalem, Edmond J. Safra Campus, Jerusalem 91904, Israel

Supporting Information

ABSTRACT: Hydrogen exchange is a powerful method to examine macromolecules. In membrane proteins, exchange can distinguish between solvent-accessible and -inaccessible residues due to shielding by the hydrophobic environment of the lipid bilayer. Herein, rather than examining which residues undergo hydrogen exchange, we employ a protocol that enables the full deuteration of all polar hydrogens in a membrane protein. We then measure the impact of hydrogen exchange on the shift of the amide I vibrational mode of individually labeled sites. The results enable us to correlate polarity with vibrational shifts, thereby providing a powerful tool to examine specific locations within a membrane protein in its native membrane environment.

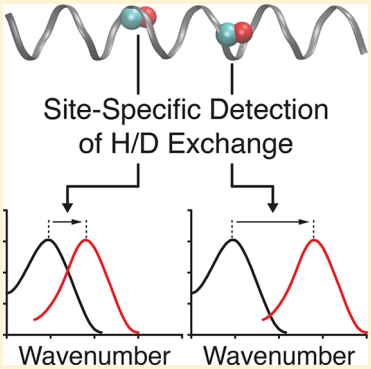

Hydrogen exchange has long been used as a tool for studying proteins.[1] The first to demonstrate that amide hydrogens may undergo exchange were Lenormant and Blout in 1953.[2] Using infrared spectroscopy, the authors concluded that the absorption in the region of 1550 cm^{-1} is partly composed of groups that can be deuterated. Soon thereafter, in a series of pioneering experiments, Linderstrøm-Lang and colleagues used hydrogen exchange for quantitative measurements and analyses of protein chemistry.[3,4] Currently, hydrogen exchange is a powerful tool for studying numerous aspects of proteins, among which insights into protein folding have been particularly informative.[5−7]

Detection of hydrogen exchange can be done using several biophysical tools that rely on the differences between the physical properties of protium and deuterium. Because protium possesses a magnetic spin of 1/2 versus deuterium with a spin of 1, the detection of hydrogen exchange rates by NMR has been particularly fruitful (for review, see ref 6). Similarly, the mass difference between the two isotopes has enabled mass spectrometry to detect hydrogen exchange with exquisite detail and sensitivity (for review, see refs 7−9). Finally, the same mass difference affects the vibrational properties of the amide group, which enables both linear[2] and multidimensional[10] IR spectroscopic approaches to monitor exchange.

The mechanism of protein amide hydrogen exchange is well characterized. It may be acid- or base-catalyzed[11] and is thought to occur via the imidic acid intermediate.[12] In either case, the reaction intermediate is charged, and, as such, amide hydrogen exchange rates increase appreciably with solvent accessibility and polarity.

Considering the above, it is of no surprise that hydrogen exchange rates in membrane proteins are considerably slower than in their water-soluble counterparts. For example, Killian and coworkers used electrospray ionization mass spectrometry to show that hydrogen exchange rates vary dramatically in a transmembrane peptide.[13] The authors attributed their results to the location of the residues, whereby water-exposed residues exhibited exchange rates that were four orders of magnitude faster than those for residues thought to be located in the hydrophobic core of the membrane. In a more recent study, Ladizhansky and colleagues, using solid-state NMR of *Anabaena* sensory rhodopsin, have shown that residues undergoing exchange are mostly confined to the solvent-exposed regions of the protein.[14] In contrast, Brooker and colleagues have demonstrated that most amide hydrogens in lactose permease are accessible to exchange, likely due to the extensive conformational fluctuations the protein undergoes.[15] Removing membrane proteins from the lipid bilayer into an organic solvent, while retaining their secondary structure, increases the hydrogen exchange rates significantly.[16,17] Of particular interest are studies examining the conformational dynamics of multipolytopic membrane proteins in which regions in the proteins exhibit ligand-dependent solvent accessibility changes.[18−22] Finally, we note that the above approach can readily be extended to the study of amphipathic peptides,[23] providing further insight into such important systems.

Received: May 30, 2018
Accepted: June 29, 2018
Published: June 29, 2018

DOI: 10.1021/acs.jpclett.8b01675
J. Phys. Chem. Lett. 2018, 9, 4059−4065

In the current study, we examine hydrogen exchange in transmembrane peptides in a site-specific manner using FTIR. Because the amide II vibrational mode is primarily due to the bending of the N−H group,[24−26] its spectral properties are sensitive to deuteration. Therefore, traditionally, FTIR has been able to provide exchange rates for membrane proteins by examining the reduction of the amide II vibrational mode.[27,28] However, such data provide only average values for the entire protein without the ability to obtain site-specific information. The reason for this is that the peak width of individual vibrations is significantly larger than the difference between contributing peaks of the amide II band, resulting in band broadening. Furthermore, ^{15}N isotopic labeling results in a -10 cm^{-1}amide II band shift[29] and is therefore insufficient for isolating individual residues.

Zanni and colleagues analyzed hydrogen exchange using 2D IR spectroscopy based on the ability of this technique to detect cross peaks between individual groups.[10] The authors made use of another isotope labeling scheme to identify individual residues: 1-$^{13}C{=}^{18}O$.[10] The dual isotope labeling shifts the peptide amide I mode (mostly the C=O stretch) by approximately -63 cm^{-1}, thereby resolving it entirely.[30,31] Subsequently, the authors have ingeniously examined cross peaks between the individual isotope-edited amide I peak and the amide II vibrational modes with 2D IR. This approach enabled Zanni and coworkers to identify the hydrogen exchange rate of a single residue by monitoring the reduction in its relevant cross peak.[10]

In the current study, a different approach is taken to study hydrogen exchange of membrane peptides in their native environment. We wish to examine the impact of hydrogen exchange on the vibrational properties of individual residues and derive structural information from such changes. Therefore, we employed 1-$^{13}C{=}^{18}O$ labels because they enable site-specific analysis of individual residues.[30,31] Furthermore, because many residues in transmembrane peptides are resistant to hydrogen exchange, we carried out the exchange process in organic solvent under acidic conditions prior to membrane reconstitution. This enabled us to obtain the spectral shifts caused by hydrogen exchange at every position in the protein, regardless of its solvent accessibility in the native state. Finally, we correlate the aforementioned shifts with the protein's known 3D structure and derive a correlation with localized polarity.

To study hydrogen exchange in a membrane environment, we examined two small, well-characterized viral membrane proteins: M2 from influenza A[32,33] and E protein from SARS coronavirus.[34−36] Analyzing two different peptides that differ in their spectral properties ensures that our results are not system-specific. In both instances we made use of peptides that encompass the transmembrane domains of the proteins and have been shown to possess many of the properties and functionalities of the full-length sequence: residues 22 to 46 in influenza M2[37,38] and residues 7 to 38 in SARS E.[39] Finally, to ease notation, protium (^1H) is designated as H, whereas deuterium (^2H) is designated as D.

It is well known that the membrane environment shields many residues from undergoing H/D exchange.[13] For example, we have shown that a peptide that encompasses the transmembrane domain of the SARS E protein undergoes H/D exchange in ca. 20% of its residues.[39] Therefore, the extent of hydrogen exchange via conventional methods, monitored by the reduction in the amide II peak (the peptidic NH deformation), may be used to gauge the percentage of the protein that is embedded in the lipid bilayer.[16,39,40] This is due to the fact that the amide II mode of a deuterated amide group is centered at 1450 cm^{-1}, as previously shown in the pioneering study of Lenormant and Blout.[2]

In the current study, rather than simply monitoring which residues underwent exchange, we sought to examine the impact of exchange on the vibrational properties of the individual amide groups. However, because exchanging the protiated water to deuterium oxide does not result in significant exchange of membrane peptides, we developed a protocol that would exchange all polar hydrogens.

In Figure 1 we depict the spectra of the SARS E protein transmembrane peptide in a lipid bilayer. Two major peaks are

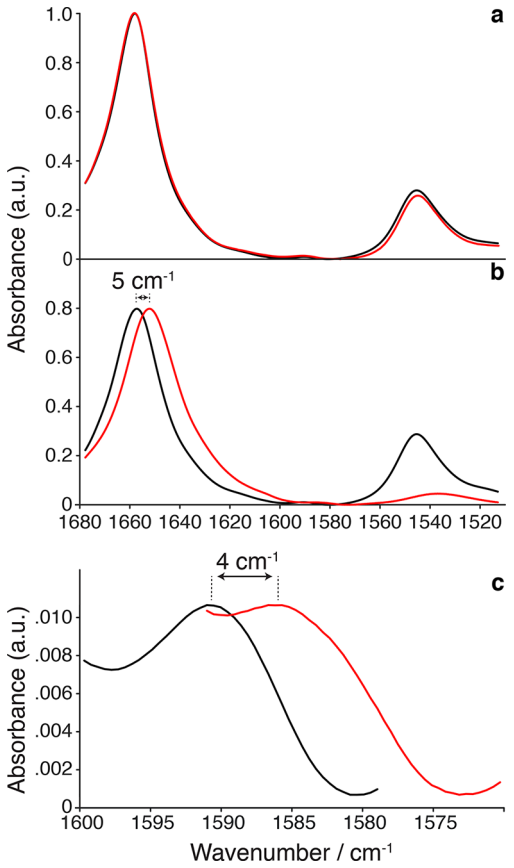

Figure 1. H/D exchange of the SARS E transmembrane peptide in a lipid bilayer. The peptide contains a single 1-$^{13}C{=}^{18}O$ label at residue Leu28. (a) Spectra obtained after purging the sample with air saturated with H_2O (black) or D_2O (red). (b) Hydrogen exchange conducted in organic solvent under acidic conditions prior to membrane reconstitution. Spectra of a protiated sample are in black, whereas spectra obtained after deuteration are in red. (c) Expansion of panel b in the region of the 1-$^{13}C{=}^{18}O$ isotope edited mode with different horizontal and vertical scales.

observed: the amide I (mostly the C=O stretch) and the amide II modes centered at 1657 and 1546 cm^{-1}, respectively. Exchanging the buffer from H_2O to D_2O results in marginal spectral changes for the SARS E protein transmembrane peptide (Figure 1a). In particular, the reduction in the amide II mode is <20%, as previously shown.[39] As stated above, this is expected because hydrogen exchange involves a charged intermediate,[12] the existence of which is strongly disfavored by the hydrophobic environment of the lipid bilayer.

DOI: 10.1021/acs.jpclett.8b01675
J. Phys. Chem. Lett. 2018, 9, 4059−4065

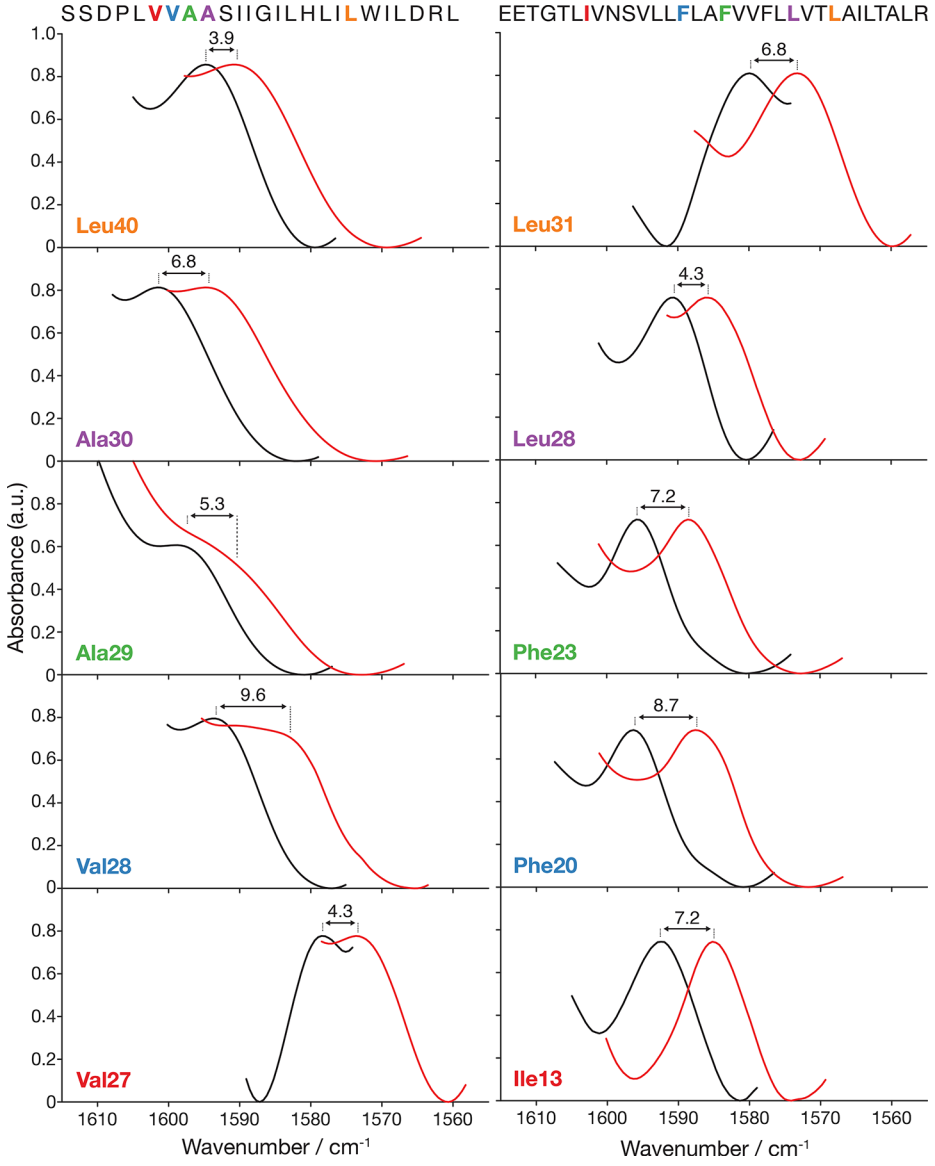

Figure 2. FTIR spectra in the region of the isotope edited amide I mode. Spectra of protiated samples are shown in black, whereas deuterated samples are in red. Influenza M2 (left) and SARS E (right) spectra were obtained with 1-^{13}C=^{18}O labeling at positions indicated in the Figure and in the color-coded sequences listed on the top. All spectra were obtained in hydrated lipid bilayers, and accurate peak positions were obtained from second derivative spectra.

To overcome the shielding effect of the lipid bilayer, we took a different approach for conducting hydrogen exchange. Membrane reconstitution takes place via organic solvent cosolubilization, followed by evaporation and hydration. Therefore, during the phase at which the peptide was dissolved in organic solvent, we used a deuterated solvent and increased the acidity with DCl to facilitate exchange. The control sample was treated identically but with protiated solvent and HCl. Finally, the results of this hydrogen exchange can be seen in Figure 1b. In this instance one can readily observe a stark reduction in the amide II peak (1546 cm^{-1}), reflecting the fact that the majority of the amide protons have undergone exchange to deuterons.

In addition to the reduction in the amide II peak, one can also observe a shift in the amide I peak, which prior to deuteration is centered at 1657 cm^{-1}. This peak arises from all of the peptide groups in the protein, and its frequency is indicative of high helical content,[41] as is known from the structure of the protein.[42] Following deuteration, the aggregate amide I band of the protein shifts to lower frequencies by 5 cm^{-1}.

The above results provide information on all of the amide groups in the protein as an average. However, because the goal of the current study was site-specific information, we needed to resort to isotopic labeling. To that end, we have included a single 1-^{13}C=^{18}O label that results in a large frequency shift of −60 cm^{-1} due to the different masses of the oscillating atoms.[30,31] Hence, one can determine the impact that deuteration has on an individual residue, which, in this instance, results in a shift to lower frequencies by 4 cm^{-1} (Figure 1c).

The ability to measure residue-specific amide I shifts upon H/D exchange prompted us to conduct a more extensive analysis. Accordingly, we measured the H/D exchange-derived shifts in five different locations in the SARS E protein and five different sites in the influenza M2 peptide. The results

DOI: 10.1021/acs.jpclett.8b01675
J. Phys. Chem. Lett. 2018, 9, 4059−4065

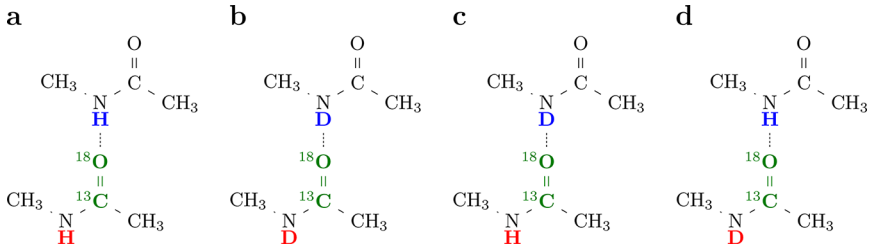

Figure 3. Model systems used for the DFT calculations of vibrational frequencies. There are two amide carbonyl groups in each system, and it is the isotopically labeled C═O (shown in green) that is participating in hydrogen bonding. Furthermore, note the distinction between the two amide hydrogens: The "hydrogen-bonding hydrogen" is in blue and the "amide hydrogen" is in red, which is part of the amide group that contains the labeled carbonyl.

presented in Figure 2, show the amide I shifts that result from H/D exchange range from 4 to 10 cm^{-1}. The average shift in the M2 peptide is 6 cm^{-1}, which is similar to that observed for the aggregate of all of the unlabeled carbonyls of the SARS peptide at 5 cm^{-1} seen in Figure 1 and slightly smaller than the SARS E shift of 6.8 cm^{-1}. The difference between the average and aggregate shifts may result from the location of the isotopic labels, as discussed in detail below.

Finally, as described in detail in the Supporting Information, we have also examined the impact of H/D exchange in a system containing a bifurcated hydrogen bond.[43] In brief, the extent of the shift in the amide I mode due to H/D exchange when the amide carbonyl is hydrogen bonded to two hydrogens is similar to systems with single hydrogen bonds.

Prior to analyzing site-specific hydrogen exchange using carbonyl labels, it was important to determine which hydrogen influences the vibrational properties of the aforementioned label. In particular, two hydrogens undergo exchange that may impact the amide I vibrational mode: the hydrogen that is bonded to the carbonyl oxygen by hydrogen bonding and the hydrogen that is part of the particular amide group.

Because it is impossible to experimentally exchange only one of the above hydrogens and not the other, we decided to conduct DFT calculations on a model system. Our configuration, shown in Figure 3, includes two *N*-methylacetamide molecules positioned such that they mimic the canonical α-helical hydrogen-bond interaction between an isotopically labeled carbonyl at position i and an amide hydrogen four residues further along in the sequence $^{13}C{=}^{18}O{\cdots}HN_{i+4}$.

To determine the impact that deuteration has on the amide I mode, we distinguish between two hydrogens: The "hydrogen-bonding hydrogen" that is hydrogen bonding to the isotopically labeled carbonyl (blue in Figure 3) and the "amide hydrogen" that is covalently attached to the labeled carbonyl as part of its amide group (red in Figure 3). Subsequently, we measured the amide I peaks in the isotopically labeled and unlabeled carbonyl groups in the different cases shown in Figure 3.

The results of the DFT calculated "hydrogen bonding" and "amide" peak shifts are shown in Table 1. In brief, the shift in frequency of the amide I vibrational mode is due to the H/D exchange of the hydrogen that is part of the amide group (red in Figure 3). In contrast, H/D exchange of the hydrogen-bonding hydrogen (blue in Figure 3) does not impact the vibrational frequency of the amide group to which it is hydrogen bonded. In other words, whereas the hydrogen that is covalently bonded to the 1-$^{13}C{=}^{18}O$ affects the amide I band upon H/D exchange, any hydrogen interacting with the carbonyl via a noncovalent bond (such as the i + 4 canonical hydrogen bond) has a negligible effect on the amide I band position upon H/D exchange.

Table 1. DFT Amide I Vibrational Peak Shifts upon H/D Exchange[a]

H/D exchange shift	amide I $^{12}C{=}^{16}O$ (cm^{-1})	amide I $^{13}C{=}^{18}O$ (cm^{-1}) (green)	models in Figure 3
hydrogen bonding H/D (blue)	3.82	0.04	**a** versus **c**
amide H/D (red)	0.02	4.60	**a** versus **d**
both H/D	3.84	4.64	**a** versus **b**

[a]Specific comparisons between the models depicted in Figure 3 are listed.

Our results are in accord with previous studies. For example, studies on the folding rates and stability of Hen Egg-White lysozyme and other proteins have shown that the deuteration does not affect the protein's stability.[44,45] More detailed analyses of model compounds by Zheng and colleagues, using ultrafast chemical exchange spectroscopy, have shown that deuteration has a negligible effect on hydrogen-bond dissociation rates.[46] Hence, the site-specific differences that we observe in the amide I vibrational shifts upon deuteration are due to the amide hydrogen.

We next decided to examine whether different structural considerations and local environments of the amide hydrogen might affect the amide I shift magnitude due to H/D exchange. Toward this end, we made use of the vibrational shifts arising from the different labels of the M2 peptides shown in Figure 2 because the known structure of the protein[47,48] affords detailed analyses at each of these sites.

To examine the electrostatic field at each of the different labeled sites, we conducted molecular dynamics simulations of the M2 tetrameric complex in a hydrated lipid bilayer. Subsequently, we could calculate the time-averaged electrostatic potential at each of the amide groups. Supporting Figure 2 depicts the results in the context of the protein structure.

However, the actual element of the electrostatic field that impacts the amide I vibrational shift is the component that is parallel to the hydrogen bond in-plane bend,[26,49] as shown in Figure 4a. The electric field of the amide amine in the in-plane bend direction was calculated by taking the negative gradient of the potential, followed by a projection onto the in-plane bend direction (see the Supporting Information). Hence, we correlated the electric field projected on the hydrogen bond in-plane bend vector to the experimentally measured amide I shifts due to H/D exchange.

DOI: 10.1021/acs.jpclett.8b01675
J. Phys. Chem. Lett. 2018, 9, 4059−4065

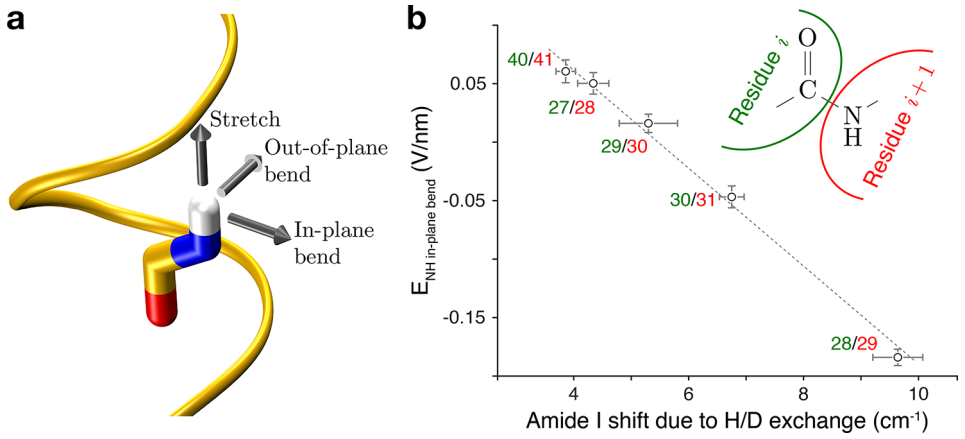

Figure 4. (a) Molecular orientation of the electric fields acting upon the amide NH. Only the NH in-plane bend contributes to amide I peak shifts. (b) Correlation between the shift in the amide I mode due to H/D exchange and the electric field acting on the amide hydrogen to cause NH in-plane bending motion. The residue number is indicated in the graph, whereby the isotopically labeled amide carbonyl of residue *i* is in green and the amine of residue *i* + 1, which is part of the same amide group, is in red (see schematic).

Gratifyingly, the electric-field component in the direction of the in-plane bend of the amide group correlates remarkably well with the extent of the hydrogen exchange shift that was obtained experimentally (Figure 4b). Specifically, the amide I shifts due to H/D exchange increase linearly with the reduction of the electric field in the direction of the in-plane bend.

An electrostatic field in the direction of the in-plane bend would downshift the amide I peak. Because D is heavier than H, any impact on the amide amine would displace a D less than an H. Hence, the shift of the amide I peak would be greater for a protiated sample than for a deuterated one. This means that the shift difference in the amide I mode due to H/D exchange would be smaller in a more polar environment, as is shown in Figure 4b.

Taken together, the extent of the shift of the amide I vibrational mode due to hydrogen exchange can be used as a gauge of the local electrostatic field. Moreover, conducting the exchange in organic solvent prior to membrane reconstitution enables one to examine every site in the protein, regardless of its native state solvent accessibility.

EXPERIMENTAL SECTION

The detailed procedures employed in the study are given in the Supporting Information. In brief, the experimental procedures used to synthesize the peptides and the isotopic labels and to collect the FTIR data are described.[43,50−52]

Hydrogen exchange was conducted in organic solvent: Lyophilized HPLC fractions containing the peptide were dissolved in fully deuterated 2,2,2-trifluoro-ethanol, acidified with DCL. Reconstitution was achieved by the addition of 1,2-dimyristoyl-*sn*-glycero-3-phosphocholine to the solution, followed by solvent evaporation and hydration with D_2O. The protiated sample was prepared in an identical manner, whereby all deuterated solvents were replaced with their protiated equivalents.

Molecular dynamics simulations were conducted as previously described[53] and expounded in detail in the Supporting Information. Similarly, DFT calculations were undertaken as previously reported[43] and described in detail in the Supporting Information.

ASSOCIATED CONTENT

Supporting Information

The Supporting Information is available free of charge on the ACS Publications website at DOI: 10.1021/acs.jpclett.8b01675.

(i) Analysis and figure depicting the impact of hydrogen exchange on the amide I vibrational mode for a peptide that contains a bifurcated hydrogen bond. (ii) Figure showing the time-averaged electrostatics in the context of the protein structure in the vicinity of the 1-^{13}C═^{18}O labeled groups. (iii) Detailed description of the materials and methods used. (PDF)

AUTHOR INFORMATION

Corresponding Authors

*E.S.B.: E-mail: esther.brielle@mail.huji.ac.il.
*I.T.A.: E-mail: arkin@huji.ac.il.

ORCID

Isaiah T. Arkin: 0000-0002-7659-1746

Notes

The authors declare no competing financial interest.

ACKNOWLEDGMENTS

This work was supported in part by grants from the Binational Science Foundation (2013618) and the Israeli Science Foundation (175/13).

REFERENCES

(1) Baldwin, R. L. Early Days of Protein Hydrogen Exchange: 1954−1972. *Proteins: Struct., Funct., Genet.* **2011**, *79*, 2021−2026.
(2) Lenormant, H.; Blout, E. R. Origin of the Absorption Band at 1,550 cm.-1 in Proteins. *Nature* **1953**, *172*, 770−771.
(3) Hvidt, A.; Linderstrøm-Lang, K. Exchange of Hydrogen Atoms in Insulin With Deuterium Atoms in Aqueous Solutions. *Biochim. Biophys. Acta* **1954**, *14*, 574−575.
(4) Hvidt, A.; Nielsen, S. O. Hydrogen Exchange in Proteins. *Adv. Protein Chem.* **1966**, *21*, 287−386.
(5) Englander, S. W. Measurement of Structural and Free Energy Changes in Hemoglobin by Hydrogen Exchange Methods. *Ann. N. Y. Acad. Sci.* **1975**, *244*, 10−27.

DOI: 10.1021/acs.jpclett.8b01675
J. Phys. Chem. Lett. 2018, 9, 4059−4065

(6) Englander, S. W.; Mayne, L. Protein Folding Studied Using Hydrogen-Exchange Labeling and Two-Dimensional NMR. *Annu. Rev. Biophys. Biomol. Struct.* **1992**, *21*, 243−265.
(7) Englander, S. W.; Mayne, L.; Kan, Z.-Y.; Hu, W. Protein Folding-How and Why: By Hydrogen Exchange, Fragment Separation, and Mass Spectrometry. *Annu. Rev. Biophys.* **2016**, *45*, 135−152.
(8) Artigues, A.; Nadeau, O. W.; Rimmer, M. A.; Villar, M. T.; Du, X.; Fenton, A. W.; Carlson, G. M. Protein Structural Analysis via Mass Spectrometry-Based Proteomics. *Adv. Exp. Med. Biol.* **2016**, *919*, 397−431.
(9) Walzthoeni, T.; Leitner, A.; Stengel, F.; Aebersold, R. Mass Spectrometry Supported Determination of Protein Complex Structure. *Curr. Opin. Struct. Biol.* **2013**, *23*, 252−260.
(10) Dunkelberger, E. B.; Woys, A. M.; Zanni, M. T. 2D IR Cross Peaks Reveal Hydrogen-Deuterium Exchange With Single Residue Specificity. *J. Phys. Chem. B* **2013**, *117*, 15297−15305.
(11) Berger, A.; Loewenstein, A.; Meiboom, S. Nuclear Magnetic Resonance Study of the Protolysis and Ionization of N-Methylacetamide1. *J. Am. Chem. Soc.* **1959**, *81*, 62−67.
(12) Perrin, C. L.; Lollo, C. P. Mechanisms of NH Proton-Exchange in Amides and Proteins - Solvent Effects and Solvent Accessibility. *J. Am. Chem. Soc.* **1984**, *106*, 2754−2757.
(13) Demmers, J. A.; Haverkamp, J.; Heck, A. J.; Koeppe, R. E., 2nd; Killian, J. A. Electrospray Ionization Mass Spectrometry as a Tool to Analyze Hydrogen/Deuterium Exchange Kinetics of Transmembrane Peptides in Lipid Bilayers. *Proc. Natl. Acad. Sci. U. S. A.* **2000**, *97*, 3189−3194.
(14) Wang, S.; Shi, L.; Kawamura, I.; Brown, L. S.; Ladizhansky, V. Site-Specific Solid-State NMR Detection of Hydrogen-Deuterium Exchange Reveals Conformational Changes in a 7-Helical Transmembrane Protein. *Biophys. J.* **2011**, *101*, L23−25.
(15) Patzlaff, J. S.; Moeller, J. A.; Barry, B. A.; Brooker, R. J. Fourier Transform Infrared Analysis of Purified Lactose Permease: A Monodisperse Lactose Permease Preparation Is Stably Folded, Alpha-Helical, and Highly Accessible to Deuterium Exchange. *Biochemistry* **1998**, *37*, 15363−15375.
(16) Arkin, I. T.; Russ, W. P.; Lebendiker, M.; Schuldiner, S. Determining the Secondary Structure and Orientation of EmrE, a Multi-Drug Transporter, Indicates a Transmembrane Four-Helix Bundle. *Biochemistry* **1996**, *35*, 7233−7238.
(17) Hansen, R. K.; Broadhurst, R. W.; Skelton, P. C.; Arkin, I. T. Hydrogen/Deuterium Exchange of Hydrophobic Peptides in Model Membranes by Electrospray Ionization Mass Spectrometry. *J. Am. Soc. Mass Spectrom.* **2002**, *13*, 1376−1387.
(18) Vahidi, S.; Bi, Y.; Dunn, S. D.; Konermann, L. Load-Dependent Destabilization of the λ-Rotor Shaft in FOF1 ATP Synthase Revealed by Hydrogen/Deuterium-Exchange Mass Spectrometry. *Proc. Natl. Acad. Sci. U. S. A.* **2016**, *113*, 2412−2417.
(19) Pan, Y.; Piyadasa, H.; O'Neil, J. D.; Konermann, L. Conformational Dynamics of a Membrane Transport Protein Probed by H/D Exchange and Covalent Labeling: The Glycerol Facilitator. *J. Mol. Biol.* **2012**, *416*, 400−413.
(20) Pirrone, G. F.; Iacob, R. E.; Engen, J. R. Applications of Hydrogen/Deuterium Exchange MS From 2012 to 2014. *Anal. Chem.* **2015**, *87*, 99−118.
(21) Forest, E.; Man, P. Conformational Dynamics and Interactions of Membrane Proteins by Hydrogen/Deuterium Mass Spectrometry. *Methods Mol. Biol.* **2016**, *1432*, 269−279.
(22) Eisinger, M. L.; Doerrbaum, A. R.; Michel, H.; Padan, E.; Langer, J. D. Ligand-Induced Conformational Dynamics of the Escherichia Coli Na+/H+ Antiporter NhaA Revealed by Hydrogen/Deuterium Exchange Mass Spectrometry. *Proc. Natl. Acad. Sci. U. S. A.* **2017**, *114*, 11691−11696.
(23) Mattila, K.; Kinder, R.; Bechinger, B. The Alignment of a Voltage-Sensing Peptide in Dodecylphosphocholine Micelles and in Oriented Lipid Bilayers by Nuclear Magnetic Resonance and Molecular Modeling. *Biophys. J.* **1999**, *77*, 2102−2113.
(24) FRASER, R. D. B.; PRICE, W. C. Infra-Red Dichroism and Protein Structure. *Nature* **1952**, *170*, 490−491.
(25) Krimm, S.; Bandekar, J. Vibrational Spectroscopy and Conformation of Peptides, Polypeptides, and Proteins. *Adv. Protein Chem.* **1986**, *38*, 181−364.
(26) Bandekar, J. Amide Modes and Protein Conformation. *Biochim. Biophys. Acta, Protein Struct. Mol. Enzymol.* **1992**, *1120*, 123−143.
(27) Vigano, C.; Manciu, L.; Buyse, F.; Goormaghtigh, E.; Ruysschaert, J. M. Attenuated Total Reflection IR Spectroscopy as a Tool to Investigate the Structure, Orientation and Tertiary Structure Changes in Peptides and Membrane Proteins. *Biopolymers* **2000**, *55*, 373−380.
(28) Vigano, C.; Smeyers, M.; Raussens, V.; Scheirlinckx, F.; Ruysschaert, J. M.; Goormaghtigh, E. Hydrogen-Deuterium Exchange in Membrane Proteins Monitored by IR Spectroscopy: A New Tool to Resolve Protein Structure and Dynamics. *Biopolymers* **2004**, *74*, 19−26.
(29) Beer, M.; Kessler, H. B.; Sutherland, G. B. B. M. Spectra of Homologous Series of Monosubstituted Amides. *J. Chem. Phys.* **1958**, *29*, 1097−1104.
(30) Torres, J.; Kukol, A.; Goodman, J. M.; Arkin, I. T. Site-Specific Examination of Secondary Structure and Orientation Determination in Membrane Proteins: The Peptidic (13)C = (18)O Group as a Novel Infrared Probe. *Biopolymers* **2001**, *59*, 396−401.
(31) Torres, J.; Adams, P. D.; Arkin, I. T. Use of a New Label, 13C = 18O, in the Determination of a Structural Model of Phospholamban in a Lipid Bilayer. Spatial Restraints Resolve the Ambiguity Arising From Interpretations of Mutagenesis Data. *J. Mol. Biol.* **2000**, *300*, 677−685.
(32) Lamb, R. A.; Lai, C. J.; Choppin, P. W. Sequences of mRNAs Derived From Genome RNA Segment 7 of Influenza Virus: Colinear and Interrupted mRNAs Code for Overlapping Proteins. *Proc. Natl. Acad. Sci. U. S. A.* **1981**, *78*, 4170−4174.
(33) Lamb, R. A.; Choppin, P. W. Identification of a Second Protein (M2) Encoded by RNA Segment 7 of Influenza Virus. *Virology* **1981**, *112*, 729−737.
(34) Marra, M. A.; Jones, S. J. M.; Astell, C. R.; Holt, R. A.; Brooks-Wilson, A.; Butterfield, Y. S. N.; Khattra, J.; Asano, J. K.; Barber, S. A.; Chan, S. Y.; et al. The Genome Sequence of the SARS-Associated Coronavirus. *Science* **2003**, *300*, 1399−1404.
(35) Rota, P. A.; Oberste, M. S.; Monroe, S. S.; Nix, W. A.; Campagnoli, R.; Icenogle, J. P.; Peñaranda, S.; Bankamp, B.; Maher, K.; Chen, M.-H.; et al. Characterization of a Novel Coronavirus Associated With Severe Acute Respiratory Syndrome. *Science* **2003**, *300*, 1394−1399.
(36) Shen, X.; Xue, J.-H.; Yu, C.-Y.; Luo, H.-B.; Qin, L.; Yu, X.-J.; Chen, J.; Chen, L.-L.; Xiong, B.; Yue, L.-D.; et al. Small Envelope Protein E of SARS: Cloning, Expression, Purification, CD Determination, and Bioinformatics Analysis. *Acta Pharmacol. Sin.* **2003**, *24*, 505−511.
(37) Duff, K. C.; Kelly, S. M.; Price, N. C.; Bradshaw, J. P. The Secondary Structure of Influenza a M2 Transmembrane Domain. A Circular Dichroism Study. *FEBS Lett.* **1992**, *311*, 256−258.
(38) Duff, K. C.; Ashley, R. H. The Transmembrane Domain of Influenza a M2 Protein Forms Amantadine-Sensitive Proton Channels in Planar Lipid Bilayers. *Virology* **1992**, *190*, 485−489.
(39) Arbely, E.; Khattari, Z.; Brotons, G.; Akkawi, M.; Salditt, T.; Arkin, I. T. A Highly Unusual Palindromic Transmembrane Helical Hairpin Formed by SARS Coronavirus E Protein. *J. Mol. Biol.* **2004**, *341*, 769−779.
(40) Arkin, I. T.; Sukharev, S. I.; Blount, P.; Kung, C.; Brünger, A. T. Helicity, Membrane Incorporation, Orientation and Thermal Stability of the Large Conductance Mechanosensitive Ion Channel From E. *Biochim. Biophys. Acta, Biomembr.* **1998**, *1369*, 131−140.
(41) Byler, D. M.; Susi, H. Examination of the Secondary Structure of Proteins by Deconvolved FTIR Spectra. *Biopolymers* **1986**, *25*, 469−487.
(42) Surya, W.; Li, Y.; Torres, J. Structural Model of the SARS Coronavirus E Channel in LMPG Micelles. *Biochim. Biophys. Acta, Biomembr.* **2018**, *1860*, 1309−1317.

DOI: 10.1021/acs.jpclett.8b01675
J. Phys. Chem. Lett. 2018, 9, 4059−4065

(43) Feldblum, E. S.; Arkin, I. T. Strength of a Bifurcated H Bond. *Proc. Natl. Acad. Sci. U. S. A.* **2014**, *111*, 4085−4090.
(44) Parker, M. J.; Clarke, A. R. Amide Backbone and Water-Related H/D Isotope Effects on the Dynamics of a Protein Folding Reaction. *Biochemistry* **1997**, *36*, 5786−5794.
(45) Itzhaki, L. S.; Evans, P. A. Solvent Isotope Effects on the Refolding Kinetics of Hen Egg-White Lysozyme. *Protein Sci.* **1996**, *5*, 140−146.
(46) Ge, C.; Shen, Y.; Deng, G.-H.; Tian, Y.; Yu, D.; Yang, X.; Yuan, K.; Zheng, J. Negligible Isotopic Effect on Dissociation of Hydrogen Bonds. *J. Phys. Chem. B* **2016**, *120*, 3187−3195.
(47) Stouffer, A. L.; Acharya, R.; Salom, D.; Levine, A. S.; Di Costanzo, L.; Soto, C. S.; Tereshko, V.; Nanda, V.; Stayrook, S.; DeGrado, W. F. Structural Basis for the Function and Inhibition of an Influenza Virus Proton Channel. *Nature* **2008**, *451*, 596−599.
(48) Thomaston, J. L.; Alfonso-Prieto, M.; Woldeyes, R. A.; Fraser, J. S.; Klein, M. L.; Fiorin, G.; DeGrado, W. F. High-Resolution Structures of the M2 Channel From Influenza a Virus Reveal Dynamic Pathways for Proton Stabilization and Transduction. *Proc. Natl. Acad. Sci. U. S. A.* **2015**, *112*, 14260−14265.
(49) Miyazawa, T.; Shimanouchi, T.; Mizushima, S. Normal Vibrations of NMethylacetamide. *J. Chem. Phys.* **1958**, *29*, 611−616.
(50) Manor, J.; Mukherjee, P.; Lin, Y.-S.; Leonov, H.; Skinner, J. L.; Zanni, M. T.; Arkin, I. T. Gating Mechanism of the Influenza a M2 Channel Revealed by 1D and 2D IR Spectroscopies. *Structure* **2009**, *17*, 247−254.
(51) Manor, J.; Feldblum, E. S.; Zanni, M. T.; Arkin, I. T. Environment Polarity in Proteins Mapped Noninvasively by FTIR Spectroscopy. *J. Phys. Chem. Lett.* **2012**, *3*, 939−944.
(52) Manor, J.; Arbely, E.; Beerlink, A.; Akkawi, M.; Arkin, I. T. Use of Isotope-Edited FTIR to Derive a Backbone Structure of a Transmembrane Protein. *J. Phys. Chem. Lett.* **2014**, *5*, 2573−2579.
(53) Leonov, H.; Astrahan, P.; Krugliak, M.; Arkin, I. T. How Do Aminoadamantanes Block the Influenza M2 Channel, and How Does Resistance Develop? *J. Am. Chem. Soc.* **2011**, *133*, 9903−9911.

DOI: 10.1021/acs.jpclett.8b01675
J. Phys. Chem. Lett. 2018, 9, 4059−4065